

A HIGH RESOLUTION METHOD OF SOURCE LOCALIZATION IN NEAR-FIELD BY USING FOCUSING TECHNIQUE

Hongyang He, Yide Wang and Joseph Saillard

Laboratoire IREENA/Ecole Polytechnique de l'Université de Nantes
Rue Christian Pauc, BP 50609, 44306 Nantes Cedex 3, France
phone: + (33) 240 683 264, email: hongyang.he@etu.univ-nantes.fr

ABSTRACT

In this paper, we present a new high resolution algorithm to localize multiple sources in near-field. After focusing on a pre-estimated location, the covariance matrix of the received signal is found to have the same structure as in the far-field situation, which allows the estimation of bearing with far-field subspace methods. With the estimated bearing, the range estimation of each source is consequently obtained by using 1-D MUSIC method without parameter pairing. This algorithm does not require a high cost 2-D search or high-order statistics, and has high-resolution performance in contrast with other fast near-field approaches. Monte Carlo simulations are used to test the performances of this approach.

Index terms— Array signal processing, Direction of arrival estimation, Position measurement, Focusing

1. INTRODUCTION

In the last two decades, subspace-based methods for estimating the directions of arrival (DOA) of far-field sources impinging on an array of sensors have become very popular. For example, the MUSIC algorithm and its derivatives have received much attention. Most of these methods make the assumption that the sources are located relatively far from the array so that the waves emitted by the sources can be considered as plane waves. With this assumption, each signal wavefront can be characterized by a single DOA. However, when a source is located close to the array (i.e., near-field), the wavefront must be characterized by both the azimuth and range. Methods based on the far-field assumption are no longer applicable to this situation. The near-field situation can occur, for example, in sonar, electronic surveillance, and seismic exploration.

Several subspace-based methods have been developed for the estimation of near-field parameters. For example, a multi-dimensional MUSIC method was proposed in [1], and [2] presented a high-order subspace-based method for wide-band sources. Considering the computational complexity due to multi-dimensional search or high-order statistics computation involved in most of the above algorithms, more recently, W. Zhi proposed a method to transform 2-D search to 1-D search via symmetric sub-arrays in [4]. By applying Fresnel approximation, the received signal model in near-field is decomposed into a far-field part and a near-field part. Based on symmetric array configuration, far-field-like rotational invariance property is found in the near-field part, which allows the bearing estimation by an ESPRIT-like method with spectral peak searching. The range is obtained by implementing 1-D MUSIC for each estimated bearing.

In this paper we propose a method with ULA to localize multiple near-field sources. The received signal model

is first divided into two parts. By using focusing technique, the near-field part of the received signal model is approximately eliminated. Consequently, far-field DOA algorithms can be employed for the bearing estimation without spectral peak searching. The range is then estimated with 1-D MUSIC method. Similar to the focusing technique in wide-band source localization [5], the focusing matrix is obtained from beamforming based pre-estimation which is implemented with a rough 2-D search. Based on this property, the algorithm is implemented with four steps: 1) Estimate an approximate location of the closely located sources with a beamforming-based method; 2) Apply focusing to the covariance matrix of the received signal; 3) Estimate the bearing of the sources with a far-field subspace based method; 4) With the estimated bearing, the range of each source is found with 1-D MUSIC method. This algorithm does not require high-order statistics computation, parameter pairing or symmetric array configuration, in addition, it has high resolution performance in contrast with other fast near-field methods.

2. NEAR-FIELD SIGNAL MODEL

Consider a near-field scenario of K uncorrelated narrow-band signals impinging to a $2M + 1$ -element ULA with inter-element spacing d , illustrated in Fig. 1. Let the array center be the phase reference point. The received signal at the m th sensor can be modeled as

$$x_m(t) = \sum_{k=1}^K e^{j\tau_{mk}} s_k(t) + n_m(t), \quad (1)$$

where $s_k(t)$ is the k th source signal received at the reference point, $n_m(t)$ is the additive white Gaussian noise and τ_{mk} is the phase shift associated with the propagation time delay between reference point and sensor m of the k th source signal, which is a function of source signal parameters, range r_k , angle θ_k and wavelength λ , given by

$$\tau_{mk} = \frac{2\pi}{\lambda} \left(\sqrt{r_k^2 + (md)^2} - 2r_k m d \sin \theta_k - r_k \right). \quad (2)$$

By using Taylor expansion [6], τ_{mk} can be expressed as

$$\tau_{mk} = \left(-\frac{2\pi d}{\lambda} \sin \theta_k \right) m + g(r_k, \theta_k, m), \quad (3)$$

where $g(r_k, \theta_k, m)$ is a function of r_k , θ_k and m .

Using this expression, the signal in (1) can be written as

$$x_m(t) = \sum_{k=1}^K e^{j\left(-\frac{2\pi d}{\lambda} \sin \theta_k\right)m + jg(r_k, \theta_k, m)} s_k(t) + n_m(t). \quad (4)$$

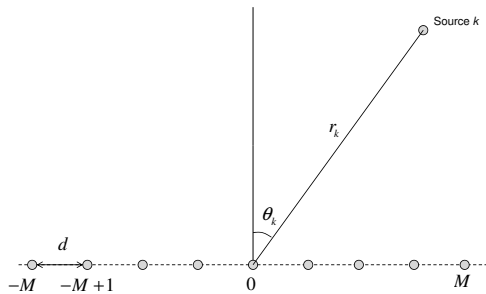


Figure 1: Near field ULA configuration

The received signal vector $\mathbf{x}(t) = [x_{-M}(t), \dots, x_M(t)]^T$ with the superscript T denoting matrix transposition can be written as

$$\mathbf{x}(t) = \mathbf{A}\mathbf{s}(t) + \mathbf{n}(t), \quad (5)$$

where $\mathbf{s}(t) = [s_1(t), \dots, s_K(t)]^T$ is the signal vector and $\mathbf{n}(t) = [n_{-M}(t), \dots, n_M(t)]^T$ is the noise vector.

The array manifold matrix \mathbf{A} is given by

$$\mathbf{A} = [\mathbf{a}(r_1, \theta_1), \dots, \mathbf{a}(r_K, \theta_K)] \quad (6)$$

with the steering vector $\mathbf{a}(r_k, \theta_k)$ being expressed as

$$\mathbf{a}(r_k, \theta_k) = \begin{bmatrix} e^{j(\frac{2\pi d}{\lambda} \sin \theta_k)M + jg(r_k, \theta_k, -M)} \\ \vdots \\ e^{j(-\frac{2\pi d}{\lambda} \sin \theta_k)M + jg(r_k, \theta_k, M)} \end{bmatrix}. \quad (7)$$

The covariance matrix of the received signal can then be written as

$$\mathbf{R}_x = E[\mathbf{x}(t)\mathbf{x}^H(t)] = \mathbf{A}\mathbf{R}_s\mathbf{A}^H + \sigma^2\mathbf{I}, \quad (8)$$

where the superscript H denotes matrix conjugate transposition, σ^2 is the power of noise, and $\mathbf{R}_s = E[\mathbf{s}(t)\mathbf{s}^H(t)]$ is the signal covariance matrix.

3. FOCUSING

We observe that the first terms of the phase elements in (7) are proportional to $\frac{2\pi d}{\lambda} \sin \theta_k$ which concerns only the direction of the source. By using focusing technique, the second term can be removed, which allows the application of far-field algorithms.

Consider that the K sources are located closely to one another. Their locations are expressed as $(r_1, \theta_1), \dots, (r_K, \theta_K)$. By using approximation, we suppose that

$$r_1 \approx r_2 \approx \dots \approx r_K = r_e$$

and

$$\theta_1 \approx \theta_2 \approx \dots \approx \theta_K = \theta_e,$$

where (r_e, θ_e) is obtained from a beamforming-based pre-estimation technique. Space frequency filter can be applied in case of K disperse sources as for the wideband focusing technique in [5], which will not be concerned in this paper.

We form a diagonal focusing matrix $\mathbf{B} \in C^{(2M+1) \times (2M+1)}$ by

$$\mathbf{B} = \begin{bmatrix} e^{-jg(r_e, \theta_e, -M)} & \dots & 0 \\ \vdots & \ddots & \vdots \\ 0 & \dots & e^{-jg(r_e, \theta_e, M)} \end{bmatrix} \quad (9)$$

where function $g(r_e, \theta_e, m)$ can be obtained from

$$g(r_e, \theta_e, m) = \left(-\frac{2\pi d}{\lambda} \sin \theta_e\right)m - \tau_{me}, \quad (10)$$

with τ_{me} being expressed as

$$\tau_{me} = \frac{2\pi}{\lambda} \left(\sqrt{r_e^2 + (md)^2} - 2r_e md \sin \theta_e - r_e \right). \quad (11)$$

The focused covariance matrix \mathbf{R}_y is given by

$$\mathbf{R}_y = \mathbf{B}(\mathbf{A}\mathbf{R}_s\mathbf{A}^H + \sigma^2\mathbf{I})\mathbf{B}^H = \mathbf{B}\mathbf{A}\mathbf{R}_s\mathbf{A}^H\mathbf{B}^H + \sigma^2\mathbf{I}. \quad (12)$$

This modified covariance matrix \mathbf{R}_y is focused at the pre-estimated location (r_e, θ_e) . It can be simplified with

$$\mathbf{C} = \mathbf{B}\mathbf{A} = [\mathbf{B}\mathbf{a}(r_1, \theta_1), \dots, \mathbf{B}\mathbf{a}(r_K, \theta_K)]. \quad (13)$$

Hence, we have

$$\mathbf{R}_y = \mathbf{C}\mathbf{R}_s\mathbf{C}^H + \sigma^2\mathbf{I}, \quad (14)$$

where \mathbf{C} is the focused array manifold matrix with its k th column being expressed as

$$\begin{aligned} \mathbf{c}_k &= \mathbf{B}\mathbf{a}(r_k, \theta_k) \\ &= \begin{bmatrix} e^{j(\frac{2\pi d}{\lambda} \sin \theta_k)M + jg(r_k, \theta_k, -M) - jg(r_e, \theta_e, -M)} \\ \vdots \\ e^{j(-\frac{2\pi d}{\lambda} \sin \theta_k)M + jg(r_k, \theta_k, M) - jg(r_e, \theta_e, M)} \end{bmatrix} \\ &\approx \begin{bmatrix} e^{j(\frac{2\pi d}{\lambda} \sin \theta_k)M} \\ \vdots \\ e^{j(-\frac{2\pi d}{\lambda} \sin \theta_k)M} \end{bmatrix}. \end{aligned} \quad (15)$$

We observe that the focused covariance matrix \mathbf{R}_y has the same structure as in far-field situation. The subspace-based method is consequently applicable for the bearing estimation.

4. SOURCE LOCALIZATION WITH FOCUSED COVARIANCE MATRIX

4.1 Eigen-Decomposition of Focused Covariance Matrix

The eigen-decomposition of the array covariance matrix \mathbf{R}_x yields

$$\mathbf{R}_x = \mathbf{U}'_s \mathbf{\Lambda}'_s \mathbf{U}'_s{}^H + \mathbf{U}'_n \mathbf{\Lambda}'_n \mathbf{U}'_n{}^H, \quad (16)$$

where $\mathbf{U}'_s \in \mathbb{C}^{(2M+1) \times K}$ contains K eigenvectors spanning the signal subspace of \mathbf{R}_x and the diagonal matrix $\mathbf{\Lambda}'_s \in \mathbb{C}^{K \times K}$ contains the corresponding eigenvalues. $\mathbf{U}'_n \in \mathbb{C}^{(2M+1) \times (2M+1-K)}$ contains $(2M+1) - K$ eigenvectors in the noise subspace of \mathbf{R}_x and the diagonal matrix $\mathbf{\Lambda}'_n \in \mathbb{C}^{(2M+1-K) \times (2M+1-K)}$ contains the corresponding eigenvalues.

Similarly, the eigen-decomposition of the focused array covariance matrix \mathbf{R}_y yields

$$\mathbf{R}_y = \mathbf{U}_s \mathbf{\Lambda}_s \mathbf{U}_s^H + \mathbf{U}_n \mathbf{\Lambda}_n \mathbf{U}_n^H, \quad (17)$$

where $\mathbf{U}_s \in \mathbb{C}^{(2M+1) \times K}$ and $\mathbf{U}_n \in \mathbb{C}^{(2M+1) \times (2M+1-K)}$ contain eigenvectors spanning the signal subspace and the noise subspace of \mathbf{R}_y respectively, and the diagonal matrix $\mathbf{\Lambda}_s \in \mathbb{C}^{K \times K}$ and $\mathbf{\Lambda}_n \in \mathbb{C}^{(2M+1-K) \times (2M+1-K)}$ contain the corresponding eigenvalues of \mathbf{R}_y .

4.2 ESPRIT for Bearing Estimation

We divide the ULA into two sub-arrays. The focused array manifold matrices for the two sub-arrays \mathbf{C}_1 and \mathbf{C}_2 can be expressed as

$$\mathbf{C} = \begin{bmatrix} \mathbf{C}_1 \\ \text{lastrow} \end{bmatrix} = \begin{bmatrix} \text{firstrow} \\ \mathbf{C}_2 \end{bmatrix}. \quad (18)$$

\mathbf{U}_s is then similarly partitioned as

$$\mathbf{U}_s = \begin{bmatrix} \mathbf{U}_{s1} \\ \text{lastrow} \end{bmatrix} = \begin{bmatrix} \text{firstrow} \\ \mathbf{U}_{s2} \end{bmatrix}. \quad (19)$$

From the signal model in (5) and the focused covariance matrix in (12), it is obvious that there exists a $K \times K$ full-rank matrix \mathbf{V} satisfying $\mathbf{U}_s = \mathbf{C}\mathbf{V}$.

Similarly, \mathbf{U}_{s1} and \mathbf{U}_{s2} corresponding to the first and second sub-array satisfy

$$\mathbf{U}_{s1} = \mathbf{C}_1 \mathbf{V} \quad (20)$$

and

$$\mathbf{U}_{s2} = \mathbf{C}_2 \mathbf{V}. \quad (21)$$

From (15), we find that the phase elements of \mathbf{c}_k are proportional to $\frac{2\pi d}{\lambda} \sin \theta_k$. Thus, \mathbf{C}_1 and \mathbf{C}_2 satisfy

$$\mathbf{C}_1 = \mathbf{C}_2 \mathbf{\Phi}, \quad (22)$$

where

$$\mathbf{\Phi} = \begin{bmatrix} e^{j(\frac{2\pi d}{\lambda} \sin \theta_1)} & \dots & 0 \\ \vdots & \ddots & \vdots \\ 0 & \dots & e^{j(\frac{2\pi d}{\lambda} \sin \theta_K)} \end{bmatrix}. \quad (23)$$

Consequently, we have

$$\mathbf{U}_{s1} = \mathbf{U}_{s2} \mathbf{V}^{-1} \mathbf{\Phi} \mathbf{V} = \mathbf{U}_{s2} \mathbf{\Psi}. \quad (24)$$

The matrix $\mathbf{\Phi}$ can be estimated by

$$\mathbf{\Phi}_{LS} = \mathbf{T}^{-1} \mathbf{\Psi} \mathbf{T} = \text{diag}(\text{eigenvalues of } \mathbf{\Psi}), \quad (25)$$

where \mathbf{T} is a full-rank square matrix and

$$\mathbf{\Psi} = (\mathbf{U}_{s2}^H \mathbf{U}_{s2})^{-1} \mathbf{U}_{s2}^H \mathbf{U}_{s1}. \quad (26)$$

Finally, the estimated bearings are obtained by

$$\hat{\theta}_k = \arcsin \left(\frac{\lambda}{2\pi d} \arg(\mathbf{\Phi}(i, i)) \right). \quad (27)$$

4.3 MUSIC for Range Estimation

By substituting the estimated angle back into the steering vectors, the localization problem is reduced to finding the parameter r in $\mathbf{a}(r, \hat{\theta}_k)$ with the received signal. The range estimation is obtained by maximizing the MUSIC spectrum $(\hat{\theta}_1, \dots, \hat{\theta}_K)$

$$\hat{r}_k = \arg \max_{r \in \mathbf{r}_e} \left[P_{MUSIC}^{(k)}(r) \right], \quad (28)$$

where \mathbf{r}_e is the region around r_e , and the MUSIC spectrum is obtained by

$$P_{MUSIC}^{(k)}(r) = \frac{1}{\mathbf{a}^H(r, \hat{\theta}_k) \mathbf{U}'_n \mathbf{U}'_n{}^H \mathbf{a}(r, \hat{\theta}_k)} \quad (29)$$

with \mathbf{U}'_n being obtained in (16).

To avoid the parameter pairing, we form the MUSIC spectrum for each estimated bearing. For K sources, K times $1 - D$ search are required for the range estimation.

4.4 Iteration

With the better estimated bearing and range in (27) and (28), we can perform the focusing technique on the covariance matrix \mathbf{R}_x for the K source separately. The focusing matrix for k th source can be expressed as

$$\mathbf{B}_{ik} = \begin{bmatrix} e^{-jg(\hat{r}_{i-1,k}, \hat{\theta}_{i-1,k}, -M)} & \dots & 0 \\ \vdots & \ddots & \vdots \\ 0 & \dots & e^{-jg(\hat{r}_{i-1,k}, \hat{\theta}_{i-1,k}, M)} \end{bmatrix}, \quad (30)$$

where the subscript ' i ' denotes the i -th iteration, $\hat{\theta}_{i-1,k}$ and $\hat{r}_{i-1,k}$ are the estimated bearing and range in the $(i-1)$ -th iteration.

The focused covariance matrix in the i -th iteration is written as

$$\mathbf{R}_y^{ik} = \mathbf{B}_{ik} \mathbf{R}_x \mathbf{B}_{ik}^H. \quad (31)$$

The better estimates of source parameters are then obtained by implementing ESPRIT and 1-D MUSIC for the K sources separately.

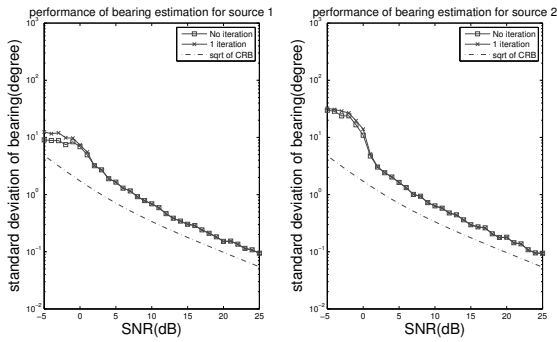


Figure 2: Standard deviation and root CRB versus SNR of the bearing estimation.

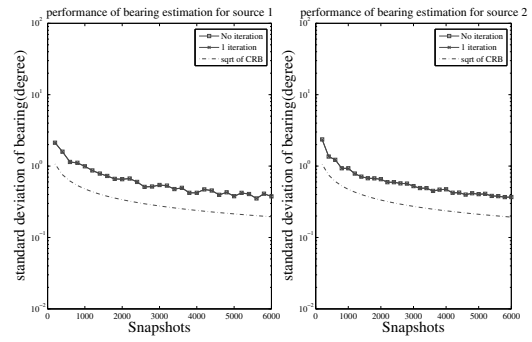


Figure 4: Standard deviation and root CRB versus snapshots of the bearing estimation.

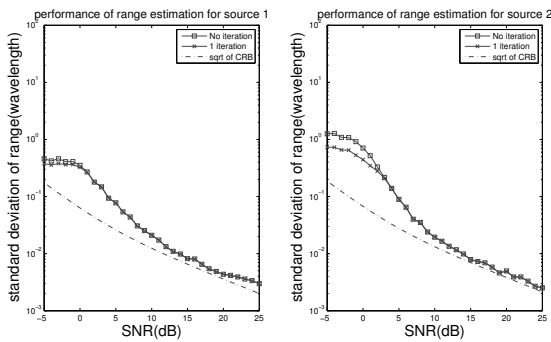


Figure 3: Standard deviation and root CRB versus SNR of the range estimation.

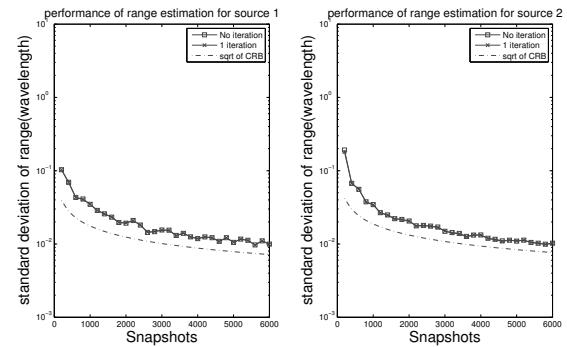


Figure 5: Standard deviation and root CRB versus snapshots of the range estimation.

5. SIMULATION RESULTS

To test the performance of the algorithm, 500 Monte Carlo simulations are performed at different SNRs (from -5dB to 25dB) and with different numbers of snapshots (from 200 to 6000). The standard deviation of the estimates is compared with the square root of the corresponding Cramer-Rao Bound (CRB) given in [6].

In this simulation, a ULA with $M = 4$ and $d = \lambda/2$ is employed to localize two uncorrelated narrow-band sources which are located closely. The noise in the simulation is additive white gaussian noise. The locations of the two sources are set as $(r_1, \theta_1) = (2.8\lambda, 32^\circ)$ and $(r_2, \theta_2) = (2.9\lambda, 28^\circ)$. The pre-estimation is obtained from the traditional beamforming method with a fast 2-D search.

Figs. 2 and 3 illustrate the standard deviation of the estimated bearing and range versus SNR, respectively. The solid lines signed by square in these figures indicate the estimated parameters without iteration, and the lines with x-mark indicate the estimated parameters from one time iteration of the algorithm. The dash-dot lines indicate the square roots of the corresponding CRBs. 2000 snapshots are used in this simulation.

Similarly, Figs. 4, 5 display the bearing and range estimation versus numbers of snapshots, respectively. The SNR is 10 dB in this simulation. From these figures, we can see that the standard deviations of estimated parameters are very close to the corresponding RCRBs, which verifies the high resolution performance of this approach.

6. CONCLUSION

Based on focusing technique, this paper proposes a high resolution algorithm for 2-D near-field multiple sources localization. By exploiting the far-field-like structure with pre-estimated parameters, the bearing and range of the sources are estimated separately. Far-field searching-free algorithms are applied to estimate the bearings and 1-D MUSIC is employed to estimate the range of each source with its estimated bearing. By implementing one time low cost 2-D search and K times 1-D search in a small region, the algorithm can localize K sources in the near field without parameter pairing. Unlike other fast near-field methods, this approach has high resolution performance.

REFERENCES

- [1] Y. D. Huang and M. Barkat, "Near-field multiple source localization by passive sensor array," *IEEE Trans. Antennas Propag.*, vol. 39, no. 7, pp. 968-975, Jul. 1991
- [2] Z. Saidi and S. Bourennane, "Cumulant-based coherent signal subspace method for bearing and range estimation," *EURASIP Journal on Advances in Signal Processing*, vol. 2007, Article ID 84576, 9 pages, doi:10.1155/2007/84576
- [3] J. C. Chen, R. E. Hudson and K. Yao, "Maximum-likelihood source localization and unknown sensor location estimation for wideband signals in the near-field,"

IEEE Trans. Signal Processing, vol. 50, pp. 1843-1854, Aug. 2002

- [4] W. Zhi and M. Y. Chia, "Near-field source localization via symmetric subarrays," *IEEE Signal Processing Letters*, vol. 14, no. 6, pp. 409-412, Jun. 2007
- [5] S. Marcos, *Les méthodes à haute résolution: traitement d'antenne et analyse spectrale*, Paris: Hermès, 1998
- [6] E. Brosicki, K. Abed-Merqim and Y. Hua, "A weighted linear prediction method for near-field source localization", *IEEE Trans. Signal Processing*, vol. 53, no. 10, pp 3651-3660, Oct. 2005